

## LMXB AND IMXB EVOLUTION: I. THE BINARY RADIO PULSAR PSR J1614-2230

JINRONG LIN<sup>1</sup>, S. RAPPAPORT<sup>1</sup>, PH. PODSIADLOWSKI<sup>2</sup>, L. NELSON<sup>3</sup>, B. PAXTON<sup>4</sup>, & P. TODOROV<sup>5</sup>

## ABSTRACT

We have computed an extensive grid of binary evolution tracks to represent low- and intermediate mass X-ray binaries (LMXBs and IMXBs). The grid includes 42,000 models which covers 60 initial donor masses over the range of  $1 - 4 M_{\odot}$  and, for each of these, 700 initial orbital periods over the range of 10 – 250 hours. These results can be applied to understanding LMXBs and IMXBs: those that evolve analogously to CVs; that form ultracompact binaries with  $P_{\text{orb}}$  in the range of 6 – 50 minutes; and that lead to wide orbits with giant donors. We also investigate the relic binary recycled radio pulsars into which these systems evolve. To evolve the donor stars in this study, we utilized a newly developed stellar evolution code called “MESA” that was designed, among other things, to be able to handle very low-mass and degenerate donors. This first application of the results is aimed at an understanding of the newly discovered pulsar PSR J1614-2230 which has a  $1.97 M_{\odot}$  neutron star,  $P_{\text{orb}} = 8.7$  days, and a companion star of  $0.5 M_{\odot}$ . We show that (i) this system is a cousin to the LMXB Cyg X-2; (ii) for neutron stars of canonical birth mass  $1.4 M_{\odot}$ , the initial donor stars which produce the closest relatives to PSR J1614-2230 have a mass between  $3.4 - 3.8 M_{\odot}$ ; (iii) neutron stars as massive as  $1.97 M_{\odot}$  are not easy to produce in spite of the initially high mass of the donor star, unless they were already born as relatively massive neutron stars; (iv) to successfully produce a system like PSR J1614-2230 requires a minimum initial neutron star mass of at least  $1.6 \pm 0.1 M_{\odot}$ , as well as initial donor masses and  $P_{\text{orb}}$  of  $\sim 4.25 \pm 0.10 M_{\odot}$  and  $\sim 49 \pm 2$  hrs, respectively; and (v) the current companion star is largely composed of CO, but should have a surface H abundance of  $\sim 10 - 15\%$ .

*Subject headings:* stars: binaries: general — stars: evolution — stars: pulsars: individual (PSR J1614-2230) — accretion, accretion disks — X-rays: binaries

## 1. INTRODUCTION

There has been an on-going effort to understand the evolution of low-mass X-ray binaries (LMXBs) since their basic nature was understood back in the late 1960’s and early 1970’s (see, e.g., Faulkner 1971; Rappaport et al. 1983; Webbink et al. 1983; Joss & Rappaport 1984; Nelson et al. 1985; Pylyser & Savonije 1988, 1989; Bhattacharya & van den Heuvel 1991; Iben et al. 1995; Podsiadlowski et al. 2002; Pfahl et al. 2003; Nelson et al. 2004; Belczynski et al. 2008). There are two rather distinct parts of the evolution to consider: (i) the formation of a neutron star in orbit with a low-mass donor star, and (ii) the subsequent portion of the evolution when mass is transferred from the companion donor star to the neutron star.

The difficulty with the first part of the evolution involves the conceptual problem of keeping the binary system bound while the massive progenitor of the neutron star (NS) explodes in a supernova event. A part of this problem was addressed by invoking a common envelope phase during which the lower-mass secondary ejects the envelope of the massive NS progenitor (Paczynski 1976; Meyer & Meyer-Hofmeister 1979;

Webbink 1979; Bhattacharya & van den Heuvel 1991). However, even this solution is not so straightforward in that there may be insufficient gravitational energy release between the inspiraling low-mass star and the core of the NS progenitor to successfully eject the envelope (see, e.g., Dewi & Tauris 2000; Pfahl et al. 2003). This difficulty could be overcome by invoking secondaries that are of intermediate mass, e.g.,  $2 - 4 M_{\odot}$  to increase the gravitational energy release (see, e.g., Pfahl et al. 2003). In turn, there has been a persistent conceptual misunderstanding that the transfer of mass from a star of  $2 - 4 M_{\odot}$  onto a  $1.4 M_{\odot}$  NS was dynamically unstable. That was shown to be untrue (Pylyser & Savonije 1988, 1989; Tauris & Savonije 1999; Podsiadlowski & Rappaport 2000; King et al. 2001; PRP02; see also Davies & Hansen 1998; King & Ritter 1999).

Starting in the 1970’s and continuing until the present, there have been numerous evolution studies of a limited number of LMXBs and IMXBs exploring the various paths which lead to very different intermediate and end-stage products. One of the more systematic was the study by Podsiadlowski et al. (2002) and Pfahl et al. (2003) which involved about 150 LMXB and IMXB systems. Given the two-dimensional parameter space of initial  $P_{\text{orb},i}$  and  $M_{2,i}$  (where  $P_{\text{orb},i}$  and  $M_{2,i}$  are the initial orbital period and mass of the donor star), the types of evolutionary paths for LMXBs or IMXBs is really quite large and varied. Possibilities include evolution to a minimum orbital period of  $\sim 70$  min with very low-mass H-rich donor stars; evolution to an ultracompact state with  $P_{\text{orb}}$  in the range of 6 – 50 minutes and He-rich donors; and evolution to wide orbits of days-to-months with low-

<sup>1</sup> 37-624B, M.I.T. Department of Physics and Kavli Institute for Astrophysics and Space Research, 70 Vassar St., Cambridge, MA, 02139; jinrongl@mit.edu; sar@mit.edu

<sup>2</sup> Department of Astrophysics, Oxford University, Oxford OX1 3RH, UK; podsi@astro.ox.ac.uk

<sup>3</sup> Department of Physics, Bishops University, Sherbrooke, QC J1M 1Z7, Canada; lnelson@ubishops.ca

<sup>4</sup> KITP, Kohn Hall, University of California at Santa Barbara, CA 93106-4030; paxton@kitp.ucsb.edu

<sup>5</sup> Laboratoire de l’Univers et ses Théories, Observatoire de Paris, 5 place Jules Janssens, F-92190 Meudon Cedex; petar.todorov@obspm.fr

mass giant donor stars.

In order to better understand the many possible evolution paths of LMXBs and IMXBs in a more systematic way, we have calculated an extensive grid of binary models encompassing 42,000 initial combinations of  $P_{\text{orb},i}$  and  $M_{2,i}$ . This is two orders of magnitude larger than the study we conducted in 2002. We took advantage of a newly developed stellar evolution code whose equations of state allow for the evolution of very low mass stars with cold dense interiors, and a cluster of computers which speeds up the overall calculation beyond what was readily available a decade ago.

With the recent discovery of PSR J1614-2230, with the most massive neutron star known ( $1.97 \pm 0.04 M_{\odot}$ ), a relatively close 8.7-day orbit, and a fairly massive white dwarf companion ( $0.5 M_{\odot}$ ), we decided to first apply our evolution calculations to understanding the origins of this system. The specific goals are to understand whether a natal NS with canonical mass of  $\sim 1.4 M_{\odot}$  can accrete sufficient material to grow to nearly  $2 M_{\odot}$ , to see whether the donor star mass is consistent with the observed  $P_{\text{orb}}$ , and to investigate how this system is related to possible progenitors in the guise of the LMXB – Cyg X-2. In all, we found  $\sim 500$  of our evolution tracks which produce systems that are at least generically related to PSR J1614-2230.

In this paper we introduce our set of binary evolution calculations which cover an extensive grid of initial orbital periods and donor masses (§2). In §3 we show how our binary evolution calculations apply directly to PSR J1614-2230. In §4 we discuss a number of the general lessons we have gleaned from this study.

## 2. OVERVIEW OF LMXB AND IMXB BINARY EVOLUTION

### 2.1. Binary Evolution Calculations

In this work we start with binary systems with an unevolved companion star in a circular orbit with an already formed neutron star of mass  $1.4 M_{\odot}$ . The prior evolution, leading to the NS and low- or intermediate-mass donor star does not concern us in this study. However, this prior phase of evolution involves a much more massive progenitor of the NS (perhaps  $8 - 15 M_{\odot}$ ), as well as a common envelope phase that unveils the He/CO core of the progenitor which, in turn, evolves to collapse and the formation of a neutron star (see, e.g., Bhattacharya & van den Heuvel 1991; Kalogera & Webbink 1998; Tauris et al. 2000; Willems & Kolb 2002, and references therein; Pfahl et al. 2003).

The subsequent evolution of the incipient LMXB or IMXB is computed with a combination of a newly developed Henyey code called “MESA” (Modules for Experiments in Stellar Astrophysics; Paxton et al. 2010) and a binary driver code. The advantages of MESA for our calculations are that (i) it is specifically designed to include equations of state that are able to handle the low-mass and high degree of degeneracy that the donor stars achieve (see Paxton et al. 2010 for details), and (ii) it is robust when used in a binary evolution code that allows for ‘hands-off’ evolution through all the various stages of the donor star and phases of mass transfer. We found that none of the evolution models failed to run to their expected completion.

The binary driver code evolves the binary orbit, including the effects of mass transfer and angular momentum losses due to gravitational radiation, magnetic braking, and possible mass ejection from the system. It keeps track of where the Roche lobe is in respect to the atmosphere of the donor star being evolved by MESA, and decides how much mass to remove from the donor star during each evolution time step. It also manages the various disparate timescales involved in the donor star as well as in the evolution of the binary orbit (details of the driver code will be presented in a future work, but its operation is very similar to that described in Madhusudhan et al. 2008). For the specific models presented here, we assumed that for sub-Eddington mass transfer rates, 90% of the mass transferred is retained by the neutron star, but that for higher transfer rates the accretion onto the NS was limited to that set by the Eddington limit. Matter ejected from the system was assumed to carry away the specific angular momentum of the neutron star.

No tidal evolution (between the donor star’s rotation and the orbital angular momentum) was incorporated in the code. We regard this as typically a  $\lesssim 10\%$  effect on the evolution, both before mass transfer commences and afterward. Magnetic braking is included (according to eq. [36] in Rappaport et al. 1983) for all stars except those that are completely convective or have a mass  $> 1.4 M_{\odot}$ . As an approximation, we also assume that magnetic braking operates even in those cases where the donor star underfills its Roche lobe and continuous synchronization between the donor star and the orbit is not guaranteed. We have verified by numerical experiment that this approximation makes little difference in the final distribution of evolution tracks shown in Fig. 1. In this work we do not consider either thermal-ionization disk instabilities or the X-ray irradiation of the donor star during the course of the evolution calculations. Their effects can be approximated via the application of after-the-fact algorithms – which we discuss in a future work. However, for the purposes of the calculations emphasized in this paper, neither effect is very important.

We computed binary evolution tracks for 42,000 LMXBs and IMXBs over a grid of 60 initial donor masses uniformly distributed over the range of  $1 - 4 M_{\odot}$  and 700 initial orbital periods distributed over the range of  $10 - 250$  hours in equal logarithmic steps. With our dense coverage of the initial binary parameter space, most of the basic types of LMXB and IMXB evolutionary tracks are explored.

The “initial orbital period” in these runs is defined as  $P_{\text{orb}}$  following the birth of the neutron star. The orbits are assumed to be circular, and the donor stars start on the ZAMS in our evolution calculations. The binary evolution is considered ‘complete’ when either (i) 10 Gyr have elapsed, or (ii) the mass transfer becomes dynamically unstable (this later condition occurs for only  $\sim 2.4\%$  of our systems, typically the ones with the largest initial donor masses and orbital periods). After the envelope of the donor star has been transferred to the neutron star (or ejected from the system), MESA continues to evolve the relic He or He/CO core of the donor until a total elapsed time of 10 Gyr has passed.

### 2.2. Results

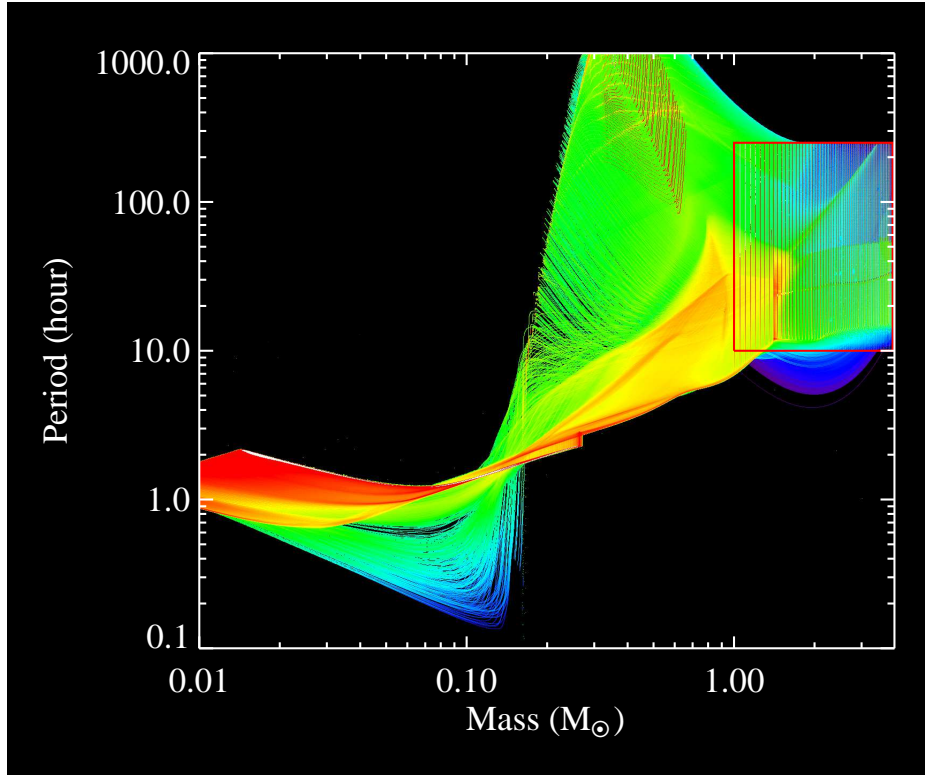


FIG. 1.— Superposed set of 38,000 binary evolution tracks in the  $P_{\text{orb}} - M_2$  plane. Each time a track crosses one of the  $1300 \times 1200$  grid points in the image, the evolution time step is stored in that pixel. The color scaling is related to the logarithm of the total system time spent in each pixel. The accumulated evolution times (per pixel) range from  $10^3$  yr for purple to  $10^{10}$  yr for red. The initial grid of models is visible in the upper right portion of the plot, outlined by a red box.

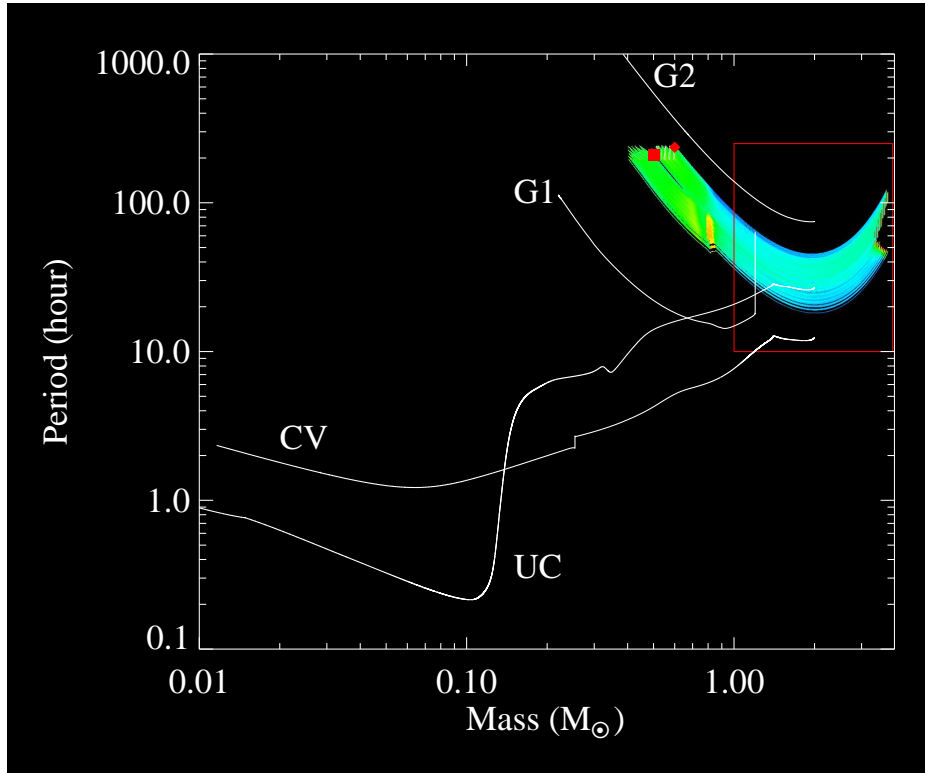


FIG. 2.— Evolution tracks of all 515 systems that terminated their evolution with  $P_{\text{orb}} = 9 \pm 1$  day, and  $M_2 = 0.5 \pm 0.1 M_{\odot}$ . The colors span cumulative evolution times (per pixel) of between  $10^4$  yr (light blue) to  $10^5$  yr (green). The small yellow region represents H-burning for up to  $3 \times 10^6$  yr (per pixel). The location of PSR J1614-2230 is marked with a red square; that of Cyg X-2 with a red diamond. The four white tracks represent other typical evolutionary paths for L/IMXBs (see text for details.)

A graphic presentation of our 38,000 binary evolution tracks, representing LMXBs and IMXBs is shown in Fig. 1 in the  $P_{\text{orb}} - M_2$  plane. We divide this plane up into  $1300 \times 1200$  discrete pixels. As the evolution tracks pass through this plane, we record, in a cumulative fashion, the evolution time that is spent in crossing a given pixel. When all the tracks have been co-added in this fashion, we display the logarithm of the total accumulated time in a pixel with color shading. The cumulative dwell times per pixel range from  $10^{10}$  yr for the red regions to  $10^3$  yr for the purple. The red box in the upper right of the diagram outlines the starting grid of initial models.

To better understand what the different types of LMXB and IMXB evolutions contribute to diagram, we show in Fig. 2 a set of illustrative individual tracks, labeled “CV”, “UC”, “G1”, and “G2”. The CV-like tracks are analogous to the evolution of cataclysmic variables, where the donor star is not very evolved at the time when mass transfer commences, remains H-rich, and gets eaten away by mass transfer until the orbital period reaches a minimum (at  $\sim 70$  min.), after which the orbit slowly expands (see, e.g., Paczynski & Sienkiewicz 1981; Rappaport et al. 1983; Howell et al. 2001, and references therein). These systems commence mass transfer for  $P_{\text{orb}}$  shorter than the so-called ‘bifurcation period’ of between  $\sim 20 - 30$  hrs (depending on the initial donor mass). The ultracompact systems (“UC”) start mass transfer in somewhat wider orbits, very near the bifurcation period, with the donor stars correspondingly more evolved, typically with H just having been depleted at the stellar center (see, e.g., Nelson et al. 1986; Tutukov et al. 1987; Pylyser & Savonije 1988, 1989; Fedorova & Ergma 1989; Podsiadlowski et al. 2002; Nelson & Rappaport 2003). Because of the high He content in the core of the donor star, these systems are able to evolve to much shorter orbital periods (some as short as 6 min.) Finally, those systems that commence mass transfer in even wider orbits (e.g., “G1” and “G2”), lead to the formation of a well-defined He core and to an increase in orbital period. For those donor stars which start with  $M_2 \lesssim 2.2 M_{\odot}$ , their degenerate cores prescribe a mass-radius relation, which in turn dictates an orbital period-core mass relation,  $P_{\text{orb}}(M_c)$ , which is clearly delineated by the locus of green terminus points in Fig. 1 which follows the  $P_{\text{orb}}(M_c)$  relation (e.g., Rappaport et al. 1995; Ergma 1996; Tauris & Savonije 1999; Nelson et al. 2004).

For donor stars with initial masses  $\gtrsim 2.2 M_{\odot}$ , however, this  $P_{\text{orb}}(M_c)$  relation does not have to be followed, and their evolution typically terminates considerably before this  $P_{\text{orb}}(M_c)$  boundary is reached. This is compounded by the fact that, due to the high mass ratios involved, the initial phases of the mass transfer, while dynamically stable, are governed by the thermal timescale of the donor star (see, e.g., King et al. 2001; Podsiadlowski & Rappaport 2000; PRP02; for further references see §3.2). These rates can therefore become greater than  $10^{-5} M_{\odot} \text{ yr}^{-1}$ , which is far in excess of the Eddington limit for a NS<sup>6</sup>. Therefore, the mass trans-

fer is highly non-conservative, and most of the mass is ejected from the system. The latter class of systems, we believe, is responsible for the evolution of both Cyg X-2 and PSR 1614-2230.

In a forthcoming paper we will concentrate on various other aspects of these evolutionary paths and describe in greater detail the various types of LMXBs and recycled pulsars that they lead to. For the present work we focus on the evolutionary paths leading to Cyg X-2-like systems and PSR J1614-2230.

### 3. BINARY EVOLUTION OF THE PSR J1614-3320 SYSTEM

#### 3.1. Properties of PSR J1614-3320

PSR J1614-2230 (Demorest et al. 2010) is a millisecond radio pulsar in an 8.7 day orbit around a (presumably) predominantly carbon-oxygen (CO) white dwarf ( $0.5 \pm 0.006 M_{\odot}$ ). The recent measurement of the Shapiro delay in PSR J1614-2230 has yielded a NS mass of  $1.97 \pm 0.04 M_{\odot}$ , making it the most massive pulsar known to date (Demorest et al. 2010). Given the constituent masses and  $P_{\text{orb}} \simeq 9$  days, this recycled pulsar system shows all the signs of having descended from an LMXB very much like Cyg X-2 ( $P_{\text{orb}} \simeq 9.8$  days,  $M_{\text{NS}} \simeq 1.8 M_{\odot}$  and  $M_2 \simeq 0.6 M_{\odot}$ ; Casares et al. 1998; Orosz & Kuulkers 1999). The orbital eccentricity of  $\sim 10^{-6}$  indicates that the evolution involved an extensive period of mass transfer via a Roche-lobe filling donor star. The characteristic spin-down age is  $\sim 5$  Gyr.

#### 3.2. Evolution Tracks Leading Close to PSR J1614-2230

Because of the very interesting and unique system parameters of PSR J1614-2230, we were motivated to search our grid of tracks for all those systems which terminate their evolution with  $P_{\text{orb}} = 9 \pm 1$  day and  $M_2 = 0.5 \pm 0.1 M_{\odot}$ . In all, there were 515 such systems; their evolution in the  $P_{\text{orb}} - M_2$  plane is shown in Fig. 2 as light blue and green tracks. Note that they all start with donor masses in the range of  $3.35 \lesssim M_{2,i} \lesssim 3.75 M_{\odot}$ , and  $P_{\text{orb},i}$  in the range of 2 - 4 days.

Note how the light blue tracks all *decrease* in  $P_{\text{orb}}$  until the donor mass reaches  $\sim 2 M_{\odot}$ , after which  $P_{\text{orb}}$  increases again until mass transfer has ceased when the donor star no longer has an extended envelope. The initial decrease in  $P_{\text{orb}}$  results from the fact that mass is being transferred from the more massive donor to the less massive NS. The total duration of the light blue portion of the tracks corresponds to a characteristic evolution time of only  $\sim$  a Myr. This rapid phase of mass transfer is referred to as “thermal timescale” mass transfer since it takes place on the thermal timescale of the radiative donor star that is more massive than the accreting NS (see, e.g., Podsiadlowski & Rappaport 2000; PRP02; for other related references see below in §3.2). Once the donor masses reach  $\sim 0.8 M_{\odot}$  the thermal timescale mass transfer is over, and the evolution slows down to timescales of tens of Myr - the nuclear evolution timescale of the donors (see the green and yellow portions of the tracks in Fig. 2).

We have selected one of these 515 tracks, as illustrative, in that its end product best matches the properties of PSR J1614-2230. We show details of that particular evolution in Fig. 3. The various panels show the evolution of  $P_{\text{orb}}$ ,  $R_2$ ,  $T_{2,\text{eff}}$ ,  $M_2$ ,  $\dot{M}$ , and information on the

<sup>6</sup> As high as these rates are, they typically remain below the rates required for the onset of ‘hypercritical accretion’ (see, e.g., Houck & Chevalier 1991) which might have allowed for the growth of higher mass neutron stars.

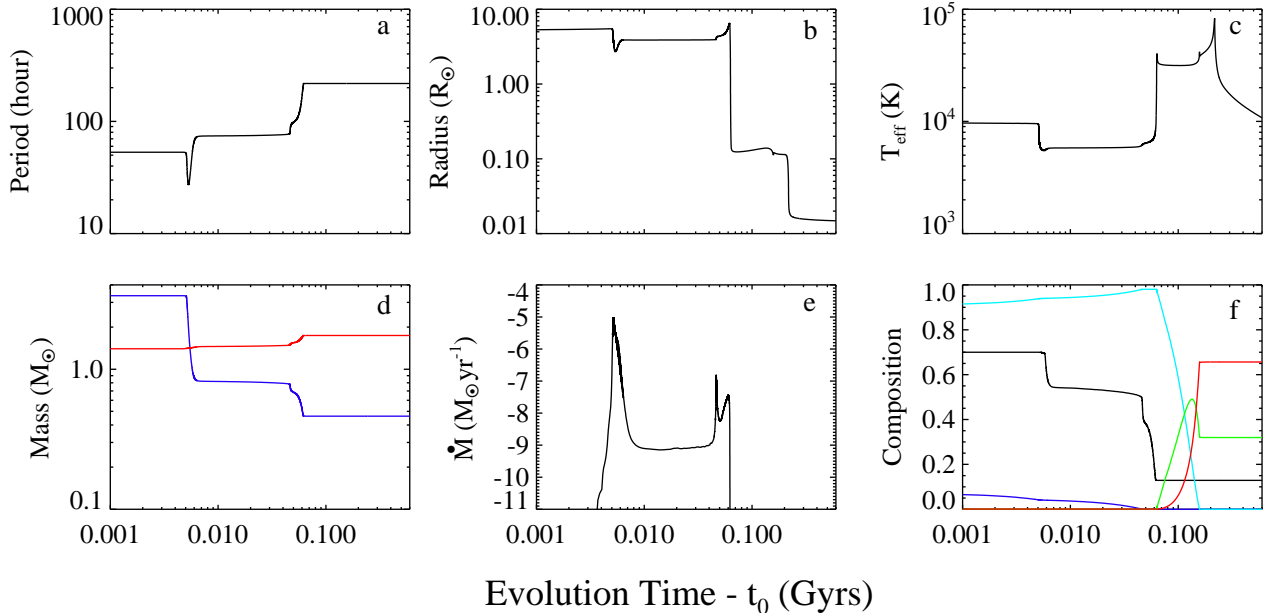


FIG. 3.— Detailed evolution vs. time of several parameters associated with the system that best represents the evolution of PSR J1614-2230 for a NS with initial mass  $1.4 M_{\odot}$  (the initial time in the plots,  $t_0$ , was chosen as 262 Myr to emphasize the mass-transfer phase). The top panels show the evolution of  $P_{\text{orb}}$ ,  $R_2$ , and  $T_{\text{eff}}$  as functions of time. The bottom panels show the evolution of stellar mass,  $\dot{M}$ , and central composition for the donor star as functions of time. In the mass panel (d) the blue and red curves are for the donor star and NS, respectively. In the composition panel blue, cyan, green, and red are the mass fractions (at the center of the donor star) of H, He, C12, and O16, respectively. The black curve is the surface H abundance.

chemical composition of the donor (star 2), as functions of the evolution time. A reference time of 262 Myr has been subtracted from the evolution time to enhance the short-timescale features around the mass-transfer phases. Note that  $\dot{M}$  refers to the mass loss rate from the donor star,

The short-lived drop in  $P_{\text{orb}}$  (panel a) corresponds to the thermal timescale mass transfer event (the large spike in  $\dot{M}$  in panel e). In panel (f) we see that the central H mass fraction is only  $\sim 6\%$  by the time mass transfer commences. The relatively long plateau in  $\dot{M}$  (panel e) at  $\sim 10^{-9} M_{\odot} \text{ yr}^{-1}$  which lasts for  $\sim 35$  Myr, corresponds to the phase of mass transfer driven by nuclear evolution during which time the remainder of the H in the core and much of the envelope is largely consumed. Once a He core has formed, there is an approximately 4-Myr interval during which H-shell burning occurs. This causes the radius of the donor star to expand from  $\sim 3.5 R_{\odot}$  to  $\sim 6 R_{\odot}$ , during which time the mass transfer rate ranges between  $10^{-8} - 10^{-7} M_{\odot} \text{ yr}^{-1}$ . The orbital period increases from  $\sim 3$  days to  $\sim 9$  days, and the donor-star mass drops to  $0.47 M_{\odot}$ . It is during this second phase of mass transfer when the accreting NS undergoes its largest growth in mass. After the H-shell burning phase, the donor star contracts, Roche lobe contact and the mass-transfer phase is over, and the He in the core of the donor star burns to C and O. The companion, which ends up being 90% C and O (with 10% of the mass in a He envelope), contracts to its final degenerate radius of  $0.015 R_{\odot}$ . This entire evolution is sometimes referred to as “case AB” since the mass transfer occurs near the end of the main sequence. (For a closely related evolution scenario for Cyg X-2 see King & Ritter 1999;

Podsiadlowski & Rappaport 2000.) and is not the same as the mass accreted by the NS.

To put the evolution of PSR J1614-2230 into some context, we show in Fig. 4 a plot of the *end points* of all the binary evolutions we ran in the plane of the final neutron-star mass vs. the final donor-star mass (now a white dwarf) – with  $P_{\text{orb},f}$  restricted to  $\gtrsim 10$  hr. In all, there are some 14,000 system end points represented in this figure. Even though the points form patterns and lie along pseudo tracks, it is important to note that they are *not* evolution tracks, but rather *end points* of numerous evolutions. These patterns result from the discrete nature of the grid of starting values for  $P_{\text{orb},i}$  and  $M_{2,i}$ . The location of PSR J1614-2230 is marked with an orange square.

The end point locations in this  $M_{\text{ns},f} - M_{2,f}$  plane are color coded according to the final value of the orbital period. The heavy green dots correspond to  $P_{\text{orb},f}$  in the range of  $8.7 \pm 1$  day, roughly commensurate with  $P_{\text{orb}}$  of PSR J1614-2230. The vertical column of heavy green dots originates from systems with initial donor-star masses  $\lesssim 2.2 M_{\odot}$  which follow the core-mass radius relation (see discussion below), and where the mass transfer rates are well below the Eddington limit. Thus, the NSs in these systems are able to grow substantially. For higher-mass donors (i.e.,  $\gtrsim 2.2 M_{\odot}$ ) that commence mass transfer near the end of the main sequence (case AB), the final NS masses lie in the range of  $\sim 2.1 - 1.65 M_{\odot}$  with white dwarf masses inversely correlated with the NS mass, and lying between  $\sim 0.26$  and  $0.50 M_{\odot}$  (the continuing line of heavy green dots). The line of systems with the most massive white dwarfs (between 0.5 and  $0.65 M_{\odot}$ ) arise from case B mass transfer (where the initial donor masses were  $> 2.2 M_{\odot}$ ), but their companion NS masses are all

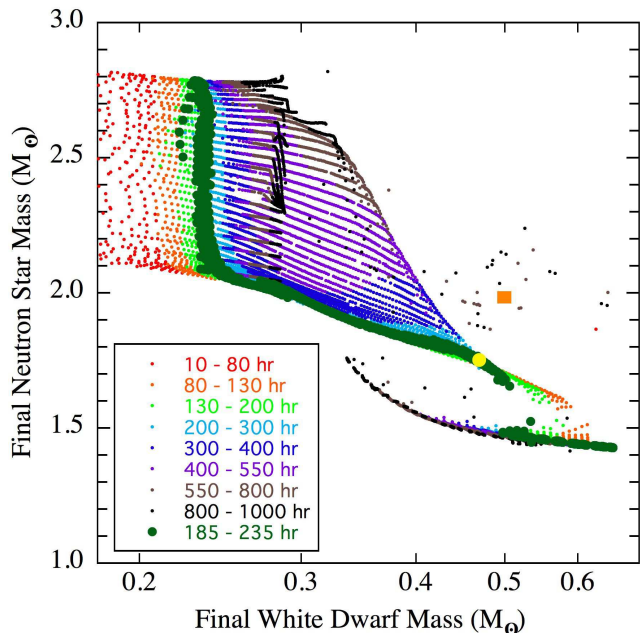


FIG. 4.— The final neutron-star mass vs. the final mass of the white dwarf companion for different ranges of final  $P_{\text{orb}}$ , as indicated by the color scaling (in hours). The dark green points are the systems with a final  $P_{\text{orb}}$  most appropriate to match PSR 1614-2230. The orange square marks the location of PSR J1614-2230, while the large yellow circle indicates the system plotted in detail in Fig. 3. Along the locus of dark green points, the higher the initial donor mass the *lower* the final neutron star mass. The bottom-most line of systems is due to case B mass transfer with initial donor masses  $\gtrsim 2.2 M_{\odot}$ . The higher mass neutron stars are very likely unphysical, and are a consequence of the high mass capture fraction assumed for sub-Eddington accretion, and not allowing these stars to collapse to black holes.

$\lesssim 1.5 M_{\odot}$ .

This ‘competition’ between the NS mass and that of the residual white dwarf companion is due to the fact that, in general, the more the donor star is evolved (hence larger core masses) when mass transfer commences, the higher is the thermal-timescale mass-transfer rate, and therefore the lower the mass retention fraction by the NS (where the Eddington limit is greatly exceeded). More specifically, the case B mass-transfer systems have only a thermal-timescale mass-transfer phase, and there is no sub-Eddington phase during which the NS mass can grow significantly. Therefore, raising an initial NS mass of  $1.4 M_{\odot}$  to  $2 M_{\odot}$  remains a difficulty for the model (see also PRP02).

The relation between the final orbital periods and the white dwarf companion masses of the systems ending with  $P_{\text{orb}} > 10$  hours is shown in Fig. 5. Again, these are 14,000 *end points*, and not evolution tracks. The location of PSR J1614-2230 is marked. The systems lying along the leftmost boundary of these end points (marked with a solid line) all represent He white dwarfs of mass between  $\sim 0.17 M_{\odot}$  and  $\sim 0.28 M_{\odot}$ . These systems form from donor stars of initial mass  $\lesssim 2.2 M_{\odot}$ , and are well represented by a nearly unique  $P_{\text{orb}}(M_c)$  relation (see, e.g., Rappaport et al. 1995; Ergma 1996; Tauris & Savonije 1999). The dashed line to the left of this set of end points is the expression given by Rappaport et al. (1995) which was already known to systematically somewhat underestimate the white dwarf mass for systems with short orbital periods below which the relationship was not de-

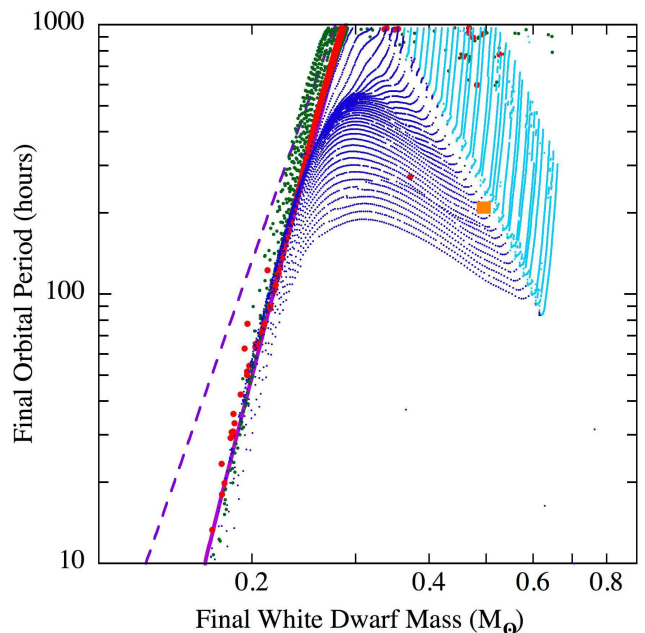


FIG. 5.— The final orbital period vs. the final mass of the white dwarf companion star for  $\sim 14,000$  systems whose final orbital period lies in the range of 10 – 1000 hr, or  $\sim 1/2$  to 40 days. The color coding of the dots is as follows: cyan and blue are for  $M_{2,i} > 2.2 M_{\odot}$  and cases B and AB, respectively (see text); the green and red represent  $M_{2,i}$  between  $1.4 - 2.2 M_{\odot}$  and  $1.0 - 1.4 M_{\odot}$ , respectively. The location of PSR J1614-2230 is marked with an orange square. The dashed purple line is the short-period, low mass end of the Rappaport et al. 1995  $P_{\text{orb}}(M_c)$  relation, while the solid purple curve is a fit to the He white dwarfs (at the left boundary) and also subsumes the Rappaport et al.  $P_{\text{orb}}(M_c)$  relation for white dwarf masses in the range of  $0.3 - 1.2 M_{\odot}$  which is off this plot. This steeper slope predicting higher-mass white dwarfs for a given  $P_{\text{orb}}$  was earlier alluded to by Tauris & Savonije (1999).

signed to work. The solid line is given by

$$P_{\text{orb}} \simeq \frac{4.6 \times 10^6 m_c^9}{(1 + 25m_c^{3.5} + 29m_c^6)^{3/2}} \text{ days} , \quad (1)$$

where  $m_c$  is the white dwarf mass expressed in solar units. We devised this expression to fit both the results shown in Fig. 5 for low-mass white dwarfs and to incorporate the expression of Rappaport et al. (1995) which extends all the way to white dwarfs of mass  $1.2 M_{\odot}$ .

The systems distinctly to the right of this  $P_{\text{orb}}(M_c)$  relation originate from donor stars with  $M_2 \gtrsim 2.2 M_{\odot}$  and do not follow the core mass-radius relation for giants. Note the ‘‘gap’’ in these more massive white dwarfs (which runs approximately at  $\sim -45^\circ$ ) dividing systems that evolved in so-called case AB (on the left side) from those that formed from somewhat more evolved donors at the time mass transfer commences, i.e., case B. These white dwarfs become progressively more CO-rich in composition toward the higher masses. (For other related studies see, e.g., Iben & Tutukov 1985; PRP02; Tauris & Savonije 1999; Han et al. 2000; Tauris et al. 2000; Nelson et al. 2004.)

Finally, in this regard, we note that PSR J1614-2230 is quite representative of the systems which started with donors of mass  $\gtrsim 2.2 M_{\odot}$  and ended up with white dwarfs of mass in the range  $0.26 - 0.65 M_{\odot}$ . The mass transfer rate in case B systems (toward the right) is so high that the neutron stars do not have much chance of growing

to interestingly high masses. By contrast, the systems to the left of the ‘gap’ between cases AB and B have intervals of near- or sub-Eddington rates which allow the highest mass NSs to be grown (see Fig. 4). In general, the higher-mass neutron stars tend to be found with the lower-mass white dwarfs.

### 3.3. Neutron Stars with Higher Initial Masses

As discussed in the previous section, none of our evolution tracks, starting with neutron stars of canonical mass  $1.4 M_{\odot}$ , produced the observed  $1.97 M_{\odot}$  NS with the requisite combination of orbital period and white dwarf mass to match the PSR J1614-2230 system. Neutron stars as massive as  $2 M_{\odot}$ , and higher, were produced with the correct orbital period, but not in combination with a massive enough white dwarf. Similarly, the orbital period and white dwarf mass combination is easy to reproduce, but not with the correct  $P_{\text{orb}}$ . We find that the final values of  $M_2$  and  $M_{\text{NS}}$  are anticorrelated when  $P_{\text{orb}}$  is fixed to  $8.7 \pm 0.5$  day. The difficulty with producing high-mass NSs in orbit with massive white dwarf companions is that the progenitors of these white dwarfs are initially substantially more massive than the NS, resulting in very rapid, thermal-timescale mass transfer (at rates as high as  $10^{-5} M_{\odot} \text{ yr}^{-1}$ ). Unless this is followed by a substantial interval of sub- or near-Eddington accretion rate, the neutron star will likely be prevented from accreting a significant fraction of the donor star’s mass.

One obvious solution to this problem of producing more massive NSs is to start with higher natal mass neutron stars. To this end, we have run a series of smaller subgrids of 700 additional starting models with initially higher-mass neutron stars. We find that the minimum required initial mass neutron star for which we could reach a final NS mass of  $1.97 M_{\odot}$  turned out to be  $1.6 M_{\odot}$ . The starting donor mass for these more ‘successful’ models, however, increased to  $\sim 4.25 \pm 0.10 M_{\odot}$  (compared to  $\sim 3.8 M_{\odot}$ ), the initial orbital periods remained near  $\sim 49 \pm 2$  hours, and the final companion CO white dwarf mass was  $\sim 0.49 M_{\odot}$ , somewhat closer to the observed value. An illustrative evolution sequence that produces a  $\sim 2 M_{\odot}$  NS, and otherwise closely resembles PSR J1614-2230, is shown in Fig. 6.

Finally, in regard to setting a limit on the mass of the natal neutron star, we note an important caveat. Throughout our calculations we adopted a very simple prescription for the Eddington-limit rate of accretion onto the neutron star of  $\dot{M}_{\text{Edd}} = 3 \times 10^{-8} M_{\odot} \text{ yr}^{-1}$ , independent of the neutron star mass or radius, or the chemical composition of the accreted material. For most of the evolutionary phases we covered in our 42,000 tracks, the accretion rate is either below  $10^{-8} M_{\odot} \text{ yr}^{-1}$ , in which case the value we choose for  $\dot{M}_{\text{Edd}}$  is unimportant, or it so high, during the thermal timescale mass-transfer phases, that the choice of  $\dot{M}_{\text{Edd}}$  also does not affect the very small fraction of mass that can be retained by the neutron star. However, for the production of systems that resemble PSR J1614-2230, with its massive neutron star and other specific properties, the largest growth of the neutron star occurs during the second phase of mass transfer in case AB evolution where  $\dot{M}$  is in the critical range of  $10^{-8} - 10^{-7} M_{\odot} \text{ yr}^{-1}$ , and where the value of  $\dot{M}_{\text{Edd}}$  very much affects how much the neutron star can

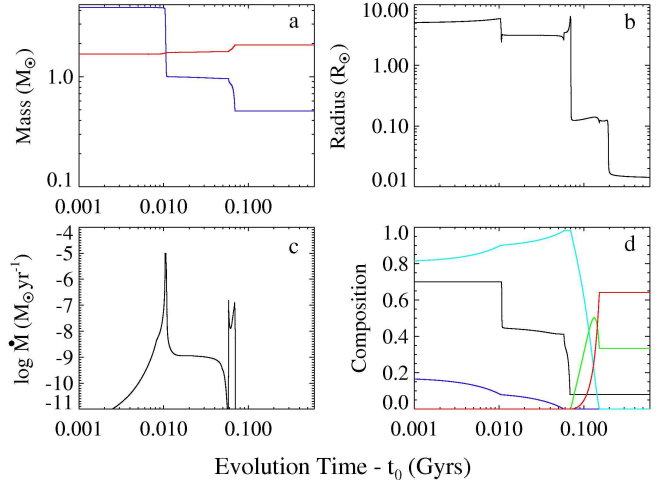


FIG. 6.— Detailed evolution vs. time of several parameters associated with the system that matches the parameters of PSR J1614-2230 for a NS with initial mass  $1.6 M_{\odot}$  and donor star of initial mass of  $4.25 M_{\odot}$ . As in Fig. 3  $t_0$  is an initial time that is subtracted off so as to emphasize the mass-transfer phase. The top panels show the evolution of the stellar masses, and the radius of the donor star, while the bottom panels show the evolution of  $\dot{M}$ , and the central composition of the donor star. The color coding in the mass curves and chemical composition are the same as in Fig. 3. The final masses of the neutron star and white dwarf in this sequence were  $1.95 M_{\odot}$  and  $0.49 M_{\odot}$ , respectively, and the final orbital period (not shown) was 206 hours (8.4 days).

grow. Adjusting the value of  $\dot{M}_{\text{Edd}}$  to be ‘‘more correct’’ is complicated by the following issues: (i) the unknown radius of the NS (by a factor of  $\sim 50\%$ ), (ii) general relativistic corrections (of  $\sim 20\%$ ), (iii) unknown allowed factors by which the Eddington limit may be violated in NS accretion (of  $\sim$  factors of 2), and (iv) changes in chemical composition of the accreted material – which is especially important as the material becomes He-rich later in the evolution. Also, the amount of mass gained by the NS is only some  $\sim 80\%$  of what was transferred through the accretion disk due to the loss of rest mass that is radiated away. Taking all these factors into account, we have run a range of tests and have concluded that such effects and their uncertainties, lead to an uncertainty in the minimum mass for a neutron star to reach  $1.97 M_{\odot}$  of  $\sim \pm 0.1 M_{\odot}$ . Therefore, the range of required minimum neutron star masses could conceivably be expanded to  $1.6 \pm 0.1 M_{\odot}$ .

## 4. SUMMARY AND CONCLUSIONS

We have used MESA to compute a large grid of 42,000 binary evolution models for LMXBs and IMXBs. We showed the broad sweep of possible evolutions, from systems which attain orbital periods as short as 6 minutes to those which grow to long-period binaries with giant donor stars. We leave a detailed discussion of the bulk of these results for a future paper. Here we have focused on what we can learn about the evolutionary paths to the newly discovered binary pulsar, PSR J1614-2230. We have selected a subset of the evolution models (515 in total) which lead to systems like PSR J1614-2230 and its evolutionary cousin, Cyg X-2, to examine in more detail. In particular, we show how an orbital period of 8.7-days can be easily understood, as can the  $0.5 M_{\odot}$  companion star. We show that for the proposed scenario, the degenerate companion star is mostly (i.e., 90%) C and

O (with a surrounding shell of He which comprises 10% of the white-dwarf mass), but there is also a thin outer envelope that is composed of  $\sim 15\%$  H.

We found, however, that starting with neutron stars of canonical mass  $1.4 M_{\odot}$ , we were not able to produce the observed  $1.97 M_{\odot}$  NS with the requisite combination of orbital period *and* white dwarf mass to match the PSR J1614-2230 system. We were able to evolve neutron stars as massive as  $2 M_{\odot}$ , with the correct orbital period, but not in combination with a massive enough white dwarf. Also, the orbital period and white dwarf mass combination was easy to generate, but not with the correct  $P_{\text{orb}}$ . As discussed above, the difficulty with evolving high-mass NSs in orbit with massive white dwarf companions is that the progenitors of these white dwarfs are initially substantially more massive than the NS, resulting in very rapid, thermal-timescale mass transfer (greatly in excess of the Eddington limit), and the neutron star is thereby prevented from accreting a significant fraction of the donor star's mass.

At this time, we are therefore tentatively led to conclude that the initial mass of the NS would have to have been higher than the canonical value of  $1.4 M_{\odot}$  in order to declare that the binary evolution of this system is fully understood. By running some 700 supplementary models with initially higher-mass NSs, we found that to successfully produce a system like PSR J1614-2230 requires a minimum initial neutron star mass of at least  $1.6 \pm 0.1 M_{\odot}$ , as well as initial donor masses and  $P_{\text{orb}}$  of  $\sim 4.25 \pm 0.10 M_{\odot}$  and  $\sim 49 \pm 2$  hrs, respectively.

For completeness in regard to producing high neutron-star masses, we point out that a number of the dynamically stable case B evolution tracks that we have generated yield mass transfer rates in excess of several times  $10^{-4} M_{\odot} \text{ yr}^{-1}$  that last for intervals of several thousand years. If ‘hypercritical accretion’, where the gravitational energy is carried off in neutrinos and the Eddington limit is thereby circumvented, is able to occur during these intervals (see, e.g., Houck & Chevalier 1991; Brown et al. 2000), then perhaps there is a chance for the neutron stars to grow during this phase of the evolution. However, it is not clear to us that the hypercritical accretion scenario, which was developed for spherical accretion onto a neutron star, would be applicable to accretion via a disk (but, see Moreno Méndez et al. 2008).

A more general conclusion from this L/IMXB study is that there is a subclass of systems which start with intermediate mass donor stars (of  $\gtrsim 2.2 M_{\odot}$ ), with  $P_{\text{orb}}$  well above the ‘bifurcation period’ (in the range of 2 – 4 days), which leads to systems like Cyg X-2 and PSR

J1614-2230. Such systems terminate their mass transfer before the donor star develops a degenerate core, and they end up with  $P_{\text{orb}}$  well below the  $P_{\text{orb}}(M_c)$  relation. (See also Iben & Tutukov 1985; PRP02; Han et al. 2000; Tauris et al. 2000).

Another important general lesson that we can take from this broad look at L/IMXB evolution is that *intermediate*-mass donor stars can evolve to virtually all the known types of LMXB systems that exist at the current epoch. These include CV-like evolution paths, ultracompact X-ray binaries, and systems with giant donor stars. This is an important finding because it is significantly easier for intermediate-mass stars to successfully eject the envelope of their massive companion progenitors of the NSs, and then remain bound during the ensuing supernova explosion.

Finally, we have provided a perspective on where in the  $P_{\text{orb}}$  and white dwarf mass plane we can expect to find the He white dwarfs that follow the  $P_{\text{orb}}(M_c)$  relation, as well as where the systems with the most massive neutron stars should be found. Depending on the upper mass limit to a neutron star,  $M_{\text{ns,max}}$ , Fig. 4 shows that there should be a fair number of black holes with mass between  $M_{\text{ns,max}}$  and  $\sim 2.8 M_{\odot}$  in binaries with He or He/CO white dwarfs that range between  $\sim 0.2$  and  $0.4 M_{\odot}$  and with orbital periods in the range of 1 – 40 days. One way to detect such important relics of stellar evolution is to search for white dwarfs with interestingly high orbital velocities (i.e.,  $v \simeq 300 (P_{\text{orb}}/\text{days}) \text{ km s}^{-1}$ ) and unseen companions. An important caveat to this is that if such low-mass black holes form in significant numbers in LMXBs that are still undergoing mass transfer, they would be directly detected by their accretion. However, there is no evidence for LMXBs with low-mass black holes (see, e.g., Farr et al. 2010; Özel et al. 2010).

We thank Deepto Chakrabarty and Lars Bildsten for helpful discussions, and an anonymous referee for very constructive suggestions. We acknowledge the early participation in this work by Nikku Madhusudhan and Josiah Schwab. J.L. gratefully acknowledges support from NASA *Chandra* grant G09-0054X; B.P. thanks the NSF for support through grants PHY 05-51164 and AST 07-07633 (BP); and SR was supported in part by NASA *Chandra* grant TM8-9002X. We acknowledge the Réseau québécois de calcul de haute performance (RQCHP) for providing the computational facilities and we thank the Natural Sciences and Engineering Research Council of Canada and the Canada Research Chairs program for financial support (LN).

## REFERENCES

- Belczynski, K., Kalogera, V., Rasio, F. A., Taam, R. E., Zezas, A., Bulik, T., Maccarone, T. J., & Ivanova, N. 2008, *ApJS*, 174, 223
- Bhattacharya, D., & van den Heuvel, E. P. J. 1991, *Phys. Rep.*, 203, 1
- Brown, G. E., Lee, C., & Bethe, H. A. 2000, *ApJ*, 541, 918
- Casares, J., Charles, P. A., & Kuulkers, E. 1998, *ApJ*, 493, L39+
- Davies, M. B., & Hansen, B. M. S. 1998, *MNRAS*, 301, 15
- Demorest, P. B., Pennucci, T., Ransom, S. M., Roberts, M. S. E., & Hessels, J. W. T. 2010, *Nature*, 467, 1081
- Dewi, J. D. M., & Tauris, T. M. 2000, *A&A*, 360, 1043
- Ergma, E. 1996, *A&A*, 315, L17
- Farr, W. M., Sravan, N., Cantrell, A., Kreidberg, L., Bailyn, C. D., Mandel, I., & Kalogera, V. 2010, *ArXiv e-prints*
- Faulkner, J. 1971, *ApJ*, 170, L99+
- Fedorova, A. V., & Ergma, E. V. 1989, *Ap&SS*, 151, 125
- Han, Z., Tout, C. A., & Eggleton, P. P. 2000, *MNRAS*, 319, 215
- Houck, J. C., & Chevalier, R. A. 1991, *ApJ*, 376, 234
- Howell, S. B., Nelson, L. A., & Rappaport, S. 2001, *ApJ*, 550, 897
- Iben, Jr., I., & Tutukov, A. V. 1985, *ApJS*, 58, 661
- Iben, Jr., I., Tutukov, A. V., & Yungelson, L. R. 1995, *ApJS*, 100, 233
- Joss, P. C., & Rappaport, S. A. 1984, *ARA&A*, 22, 537
- Kalogera, V., & Webbink, R. F. 1998, *ApJ*, 493, 351
- King, A. R., & Ritter, H. 1999, *MNRAS*, 309, 253



- King, A. R., Schenker, K., Kolb, U., & Davies, M. B. 2001, MNRAS, 321, 327
- Madhusudhan, N., Rappaport, S., Podsiadlowski, P., & Nelson, L. 2008, ApJ, 688, 1235
- Meyer, F., & Meyer-Hofmeister, E. 1979, A&A, 78, 167
- Moreno Méndez, E., Brown, G. E., Lee, C., & Park, I. H. 2008, ApJ, 689, L9
- Nelson, L. A., Chau, W. Y., & Rosenblum, A. 1985, ApJ, 299, 658
- Nelson, L. A., Dubeau, E., & MacCannell, K. A. 2004, ApJ, 616, 1124
- Nelson, L. A., & Rappaport, S. 2003, ApJ, 598, 431
- Nelson, L. A., Rappaport, S. A., & Joss, P. C. 1986, ApJ, 304, 231
- Orosz, J. A., & Kuulkers, E. 1999, MNRAS, 305, 132
- Özel, F., Psaltis, D., Narayan, R., & McClintock, J. E. 2010, ApJ, 725, 1918
- Paczynski, B. 1976, in IAU Symposium, Vol. 73, Structure and Evolution of Close Binary Systems, ed. P. Eggleton, S. Mitton, & J. Whelan, 75–+
- Paczynski, B., & Sienkiewicz, R. 1981, ApJ, 248, L27
- Paxton, B., Bildsten, L., Dotter, A., Herwig, F., Lesaffre, P., & Timmes, F. 2010, ArXiv e-prints
- Pfahl, E., Rappaport, S., & Podsiadlowski, P. 2003, ApJ, 597, 1036
- Podsiadlowski, P., & Rappaport, S. 2000, ApJ, 529, 946
- Podsiadlowski, P., Rappaport, S., & Pfahl, E. D. 2002, ApJ, 565, 1107 (PRP02)
- Pylyser, E., & Savonije, G. J. 1988, A&A, 191, 57
- Pylyser, E. H. P., & Savonije, G. J. 1989, A&A, 208, 52
- Rappaport, S., Podsiadlowski, P., Joss, P. C., Di Stefano, R., & Han, Z. 1995, MNRAS, 273, 731
- Rappaport, S., Verbunt, F., & Joss, P. C. 1983, ApJ, 275, 713
- Tauris, T. M., & Savonije, G. J. 1999, A&A, 350, 928
- Tauris, T. M., van den Heuvel, E. P. J., & Savonije, G. J. 2000, ApJ, 530, L93
- Tutukov, A. V., Fedorova, A. V., Ergma, E. V., & Yungelson, L. R. 1987, Soviet Astronomy Letters, 13, 328
- Webbink, R. F. 1979, in IAU Colloq. 53: White Dwarfs and Variable Degenerate Stars, ed. H. M. van Horn & V. Weidemann, 426–447
- Webbink, R. F., Rappaport, S., & Savonije, G. J. 1983, ApJ, 270, 678
- Willems, B., & Kolb, U. 2002, MNRAS, 337, 1004